# High-Nuclearity Phosphinidene Clusters. Synthesis, Characterization, and Reactivity of Two $W_2Ru_4$ Clusters with a $\mu_4$-$\eta^2$-CO Ligand

Jar-Cheng Wang, Ren-Chiun Lin, and Yun Chi*

*Department of Chemistry, National Tsing Hua University,*
*Hsinchu 30043, Taiwan, Republic of China*

Shie-Ming Peng* and Gene-Hsiang Lee

*Department of Chemistry, National Taiwan University,*
*Taipei 10764, Taiwan, Republic of China*

*Received April 26, 1993*⊗

Thermolysis of the heterometallic phosphinidene cluster $Cp^*WRu_2(CO)_8(\mu\text{-}H)(\mu_3\text{-}PPh)$ (2) in refluxing toluene solution gave two $W_2Ru_4$ clusters (4 and 5) via elimination of one $H_2$ and four CO molecules. Complexes 4 and 5 are isomers, which adopt a square-pyramidal $WRu_4$ core skeleton with a pendant W atom bridging a Ru–Ru edge, on which the unusual $\mu_4$-$\eta^2$-CO ligand is associated with the butterfly $W_2Ru_2$ array; one $\mu_4$-PPh ligand occupies a $WRu_3$ square face in both isomers, while a second $\mu_3$-PPh ligand caps a $Ru_3$ face in 4 and a $WRu_2$ face in 5. In refluxing toluene solution 4 and 5 began to equilibrate via a process involving $\mu_3$-PPh migration. When a solution of 4 was treated with dihydrogen, cluster degradation occurred to regenerate a small amount of 2 and tetranuclear $Cp^*WRu_3(CO)_{10}(\mu_3\text{-}PPh)(\mu_3\text{-}H)$ (3). Similarly, compound 4 reacts with carbon monoxide at 4 atm to produce the homometallic phosphinidene compounds $Ru_3(CO)_9(\mu_3\text{-}PPh)_2$ (6) and $Ru_4(CO)_{11}(\mu_4\text{-}PPh)_2$ (7) in moderate yield. Crystal data for 4: space group $P2_1/n$; $a = 12.174(4)$, $b = 17.427(5)$, $c = 22.773(6)$ Å; $\beta = 100.21(2)°$; $Z = 4$; 5016 observed reflections; $R = 0.034$. Crystal data for 5: space group $C2/c$; $a = 45.527(5)$, $b = 10.201(1)$, $c = 21.906(9)$ Å, $\beta = 93.90(3)°$; $Z = 8$; 5448 observed reflections; $R = 0.033$.

## Introduction

It is well established that trinuclear complexes with a bridging heteroatom ligand undergo cluster condensation to afford high-nuclearity cluster compounds on thermolysis or UV irradiation.[1] The success of this method relies on a proposal that the nonmetal bridging ligands, such as sulfido,[2] phosphido, or phosphinidene[3] ligands, can stabilize the cluster framework through multisite interaction with metal atoms, thus preventing the unwanted cluster demolition[4] and promoting the capture of a second metal-containing group.[5] By following this strategy, Geoffroy and co-workers have reported the formation of the hexanuclear complex $Ru_6(CO)_{15}(\mu_4\text{-}NPh)_2$ through thermolysis of the homotrinuclear imido cluster compound $Ru_3(CO)_{10}(\mu_3\text{-}NPh)$.[6] Attempts to extend a similar pattern of reactivity to the related heterometallic nitrene cluster $LWRu_2(CO)_8(\mu\text{-}H)(\mu_3\text{-}NPh)$ (1; L = $C_5H_5$, $C_5Me_5$)[7] have failed to afford a condensation product of high nuclearity.

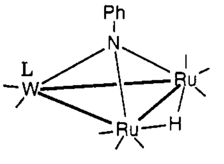

1, L = Cp, Cp*

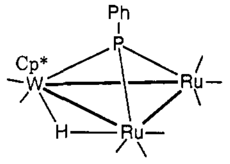

2

However, it was of interest to determine if the lack of reactivity would be observed for the respective phosphinidene form; thus, we thought to use $Cp^*WRu_2(CO)_8(\mu\text{-}H)(\mu_3\text{-}PPh)$ (2) as a precursor[8] to reinvestigate this cluster self-assembling reaction. In this paper, we describe the synthesis, reactivity, and crystal structure of two $Ru_4W_2$ clusters prepared from the condensation of 2. These newly prepared cluster compounds are of special interest because of the formation of an quadruply bonded $\eta^2$-CO ligand[9] which is associated with a local butterfly $Ru_2W_2$ arrangement. In addition, we observed that the $\eta^2$-CO ligand would not exchange with $^{13}$CO, under conditions (100 °C, 12 h) for routine $^{13}$CO enrichment. Furthermore, thermolysis of either $Ru_4W_2$ cluster gave a mixture of both isomers via a unique process involving phosphinidene migration.

## Experimental Section

**General Information and Materials.** Infrared spectra were recorded on a Perkin-Elmer 2000 FT-IR spectrometer. $^1$H and

---

⊗ Abstract published in *Advance ACS Abstracts,* September 15, 1993.

[1] (a) Adams, R. D. *Polyhedron* **1985,** *4,* 2003. (b) Vargas, M. D.; Nicholls, J. N. *Adv. Inorg. Chem. Radiochem.* **1986,** *30,* 123.

[2] Adams, R. D.; Dawoodi, Z.; Foust, D. F.; Segmuller, B. E. *J. Am. Chem. Soc.* **1983,** *105,* 831.

[3] (a) Natarajan, K.; Zsolnai, L; Huttner, G. *J. Organomet. Chem.* **1981,** *209,* 85. (b) Van Gastel, F.; Taylor, N. J.; Carty, A. J. *J. Chem. Soc., Chem. Commun.* **1987,** 1049. (c) Huttner, G.; Knoll, K. *Angew. Chem., Int. Ed. Engl.* **1987,** *26,* 743.

[4] Vahrenkamp, H. *Adv. Organomet. Chem.* **1983,** *22,* 169.

[5] Adams, R. D. In *The Chemistry of Metal Cluster Complexes;* Shriver, D. F., Kaesz, H. D., Adams, R. D., Eds.; VCH: New York, 1990; Chapter 3.

[6] Han, S.-H.; Nguyen, S. T.; Geoffroy, G. L.; Rheingold, A. L. *Organometallics* **1988,** *7,* 2034.

[7] (a) Chi, Y.; Liu, L.-K.; Huttner, G.; Zsolnai, L. *J. Organomet. Chem.* **1990,** *390,* C50. (b) Chi, Y.; Hsu, H.-F.; Liu, L.-K.; Peng, S.-M.; Lee, G.-H. *Organometallics* **1992,** *11,* 1763.

[8] Lin, R.-C.; Chi, Y.; Peng, S.-M.; Lee, G.-H. *Inorg. Chem.* **1992,** *31,* 3818.

[9] (a) Horwitz, C. P.; Shriver, D. F. *Adv. Organomet. Chem.* **1984,** *23,* 219. (b) Field, J. S.; Haines, R. J.; Jay, J. A. *J. Organomet. Chem.* **1989,** *377,* C35. (c) Chi, Y.; Chuang, S.-H.; Liu, L.-K.; Wen, Y.-S. *Organometallics* **1991,** *10,* 2485. (d) Brun, L. P.; Dawkins, G. M.; Green, M.; Miles, A. D.; Orpen, A. G.; Stone, F. G. A. *J. Chem. Soc., Chem. Commun.* **1982,** 926.

0276-7333/93/2312-4061$04.00/0

$^{31}P$ NMR spectra were recorded on a Varian Unity-400 or a Bruker AMX-300 instrument. $^{31}P$ NMR chemical shifts are quoted with respect to external standard 85% $H_3PO_4$. Mass spectra were obtained on a JEOL-HX110 instrument operating in the fast atom bombardment (FAB) mode. All reactions were performed under a nitrogen atmosphere using deoxygenated solvents dried with an appropriate reagent. The progress of reactions was monitored by analytical thin-layer chromatography (5735 Kieselgel 60 $F_{254}$, E. Merck), and the products were separated on commercially available preparative thin-layer chromatographic plates (Kieselgel 60 $F_{254}$, E. Merck). Elemental analyses were performed at the NSC Regional Instrumentation Center at National Cheng Kung University, Tainan, Taiwan.

**Thermolysis of $Cp^*WRu_2(CO)_8(\mu_3\text{-}PPh)(\mu\text{-}H)$.** A toluene solution (30 mL) of $Cp^*WRu_2(CO)_8(\mu_3\text{-}PPh)(\mu\text{-}H)$ (2; 94 mg, 0.110 mmol) was heated at reflux for 2 h, with a slow stream of $N_2$ gas passing into the solution to assist removal of dissociated CO gas. After the solution was cooled to room temperature, the solvent was evaporated in vacuo and the residue was separated by thin-layer chromatography (TLC, 1:1 dichloromethane–hexane), giving 7.5 mg of red **2** (0.008 mmol, 7%), 4 mg of $Cp^*WRu_3(CO)_{10}(\mu_3\text{-}PPh)(\mu_3\text{-}H)$ (**3**; 0.004 mmol, 3%), 52.4 mg of dark brown $Cp^*_2W_2Ru_4(CO)_{12}(\mu_4\text{-}PPh)(\mu_3\text{-}PPh)$ (**4**; 0.033 mmol, 60%), and 9 mg of a second dark brown complex, $Cp^*_2W_2Ru_4(CO)_{12}(\mu_4\text{-}PPh)(\mu_3\text{-}PPh)$ (**5**; 0.006 mmol, 10%), in order of elution. Crystals of **4** and **5** suitable for X-ray analysis were obtained by recrystallization from a layered solution of dichloromethane–methanol at room temperature.

Spectral data for **4**: MS (FAB, $^{102}Ru$, $^{184}W$) $m/z$ 1595; IR ($C_6H_{12}$) $\nu$(CO) 2051 (vw, br), 2024 (vs), 1997 (vs), 1984 (vs), 1977 (s), 1961 (s), 1953 (m), 1943 (w, sh), 1919 (w, br), 1857 (w, br) cm$^{-1}$; $^1H$ NMR ($CDCl_3$; room temperature) $\delta$ 8.12 (q, 1H, $J_{H-H} = 7$ Hz), 7.99 (q, 2H, $J_{H-H} = 8$ Hz), 7.59 (m, 3H), 7.19 (br, 4H), 1.82 (s, 15H), 1.80 (s, 15H); $^{13}C$ NMR ($CD_2Cl_2$, room temperature, CO) $\delta$ 280.5 ($J_{W-C} = 163$ Hz), 240.4 ($J_{W-C} = 178$ Hz), 230.2 ($J_{W-C} = 164$ Hz), 218.3 ($J_{W-C} = 141$ Hz), 213.6, 212.9 ($J_{P-C} = 31$ Hz), 210.6 ($J_{P-C} = 30$ Hz), 205.2 ($J_{P-C} = 10$ Hz), 200.0, 198.3, 194.8, 191.4; $^{31}P$ NMR ($CD_2Cl_2$, room temperature) $\delta$ 493.6 (d, $J_{P-P} = 41$ Hz), 376.0 (d, $J_{W-P} = 257$ Hz, $J_{P-P} = 41$ Hz). Anal. Calcd for $C_{44}H_{40}O_{12}P_2Ru_4W_2$: C, 33.14; H, 2.53. Found: C, 33.06; H, 2.47.

**Study of $^{13}CO$ Exchange.** A toluene solution (15 mL) of **4** (36 mg, 0.023 mmol) was placed into a 30-mL thick-wall sealed tube equipped with a Rotaflo stopcock. The tube was charged with 1 atm of 50% $^{13}CO$ and placed into an oil bath maintained at 100 °C for 12 h. From the reaction mixture 20 mg of **4** was recovered after TLC separation.

**Thermolysis of 4.** A toluene solution (30 mL) of **4** (30 mg, 0.020 mmol) was heated to reflux for 2 h. After the solution was cooled to room temperature, the solvent was evaporated in vacuo and the residue was separated by thin-layer chromatography (1:1 dichloromethane–hexane), giving 17 mg of **4** (0.012 mmol, 60%) and 5 mg of **5** (0.003 mmol, 17%).

Spectral data for **5**: MS (FAB, $^{102}Ru$, $^{184}W$) $m/z$ 1594; IR ($C_6H_{12}$) $\nu$(CO) 2047 (vs), 2040 (m, sh), 2035 (m, sh), 2014 (vs), 1993 (s), 1970 (s), 1958 (s), 1941 (m), 1914 (m), 1859 (br), 1783 (br) cm$^{-1}$; $^1H$ NMR ($CDCl_3$, room temperature) $\delta$ 7.74 (m, 2H), 7.55 (m, 3H), 7.16 (m, 3H), 7.01 (m, 2H), 1.96 (s, 15H), 1.77 (s, 15H); $^{13}C$ NMR ($CDCl_3$, 213 K, CO) $\delta$ 267.8 ($J_{W-C} = 175$ Hz), 246.4 ($J_{W-C} = 183$ Hz), 234.2, 219.6 ($J_{W-C} = 147$ Hz), 218.8, 210.4, 204.8 (q, $J_{P-C} = 9$ and 38 Hz), 202.2 (d, $J_{P-C} = 35$ Hz), 202.1, 193.7, 189.1, 183.8; $^{31}P$ NMR ($CDCl_3$, room temperature) $\delta$ 439.8 (d, $J_{W-P} = 342$ Hz, $J_{P-P} = 15$ Hz), 333.2 (d, $J_{W-P} = 241$ Hz, $J_{P-P} = 15$ Hz). Anal. Calcd for $C_{45}H_{42}O_{12}P_2Ru_4W_2Cl_2$: C, 32.18; H, 2.52. Found: C, 32.17; H, 2.56.

**Thermolysis of 5.** A toluene solution (30 mL) of **5** (7.5 mg, 0.005 mmol) was heated to reflux for 2 h. After the solution was cooled to room temperature, the solvent was evaporated in vacuo and the residue was separated by TLC (1:1 dichloromethane–hexane), giving approximately 1 mg of **4** (0.0006 mmol, 13%) and 6 mg of **5** (0.004 mmol, 80%).

**Reaction of 4 with Carbon Monoxide.** A toluene solution (20 mL) of **4** (56 mg, 0.035 mmol) was placed into a 250-mL thick-wall pressure bottle. The bottle was charged with 4 atm of CO gas and placed into an oil bath maintained at 100 °C. After 12 h, the solvent was evaporated and the residue was separated by TLC (1:1 dichloromethane–hexane), giving 10 mg of yellow $Ru_3(CO)_9(\mu_3\text{-}PPh)_2$ (**6**; 0.013 mmol, 37%) and 10 mg of purple $Ru_4(CO)_{11}(\mu_4\text{-}PPh)_2$, (**7**; 0.011 mmol, 30%).

Spectral data for **6**: MS (FAB, $^{102}Ru$) $m/z$ 773; IR ($C_6H_{12}$) $\nu$(CO) 2083 (w) 2061 (s), 2039 (s), 2017 (s), 2004 (s), 1994 (m), 1974 (m) cm$^{-1}$; $^{31}P$ NMR ($CDCl_3$, room temperature) $\delta$ 214 (s). Spectral data for **7**: MS (FAB, $^{102}Ru$) $m/z$ 929; IR ($C_6H_{12}$) $\nu$(CO) 2080 (m), 2045 (vs), 2038 (vs), 2022 (vs), 1987 (s), 1838 (m) cm$^{-1}$; $^{31}P$ NMR ($CDCl_3$, room temperature) $\delta$ 168 (s).

**Reaction of 4 with Hydrogen.** The toluene solution (30 mL) of **4** (50 mg, 0.031 mmol) was refluxed under 1 atm of $H_2$ for 1 h. After the solution was cooled to room temperature, the solvent was evaporated and the residue was separated by TLC (1:1 dichloromethane–hexane), giving 4.5 mg of **2** (0.004 mmol, 16%), 4 mg of **3** (0.003 mmol, 13%), and 18 mg of **4** (0.011 mmol, 35%).

**X-ray Crystallography.** Diffraction measurements were carried out on a Nonius CAD-4 diffractometer. Lattice parameters of **4** were determined from 25 randomly selected high-angle reflections with $2\theta$ angles in the range 19.52–26.88. The space group $P2_1/n$ was identified on the basis of systematic absences. All reflections were corrected for Lorentz, polarization, and absorption effects. The absorption corrections were made by the $\psi$-scan method, and the minimum and maximum transmission factors were 0.335 and 1.000, respectively. All data reduction and refinement were performed using the NRCC-SDP-VAX packages. The structures were solved by direct methods and refined by least-squares cycles; all non-hydrogen atoms were refined with anistropic thermal parameters. The hydrogen atoms of the phenyl and pentamethylcyclopentadienyl groups were calculated in idealized positions with a fixed temperature coefficient ($U_H = U_C + 0.01$ Å$^2$) and included in the structure factor calculation.

Lattice parameters of **5** were determined from 25 randomly selected high-angle reflections with $2\theta$ angles in the range 18.70–25.20; the space group $C2/c$ was identified from the systematic absences and centric intensity distribution of the data and confirmed by successfully solving the crystal structure. The absorption corrections were made by the $\psi$-scan method, and the minimum and maximum transmission factors were 0.253 and 1.000, respectively. All data reduction and refinement were performed using the NRCC-SDP-VAX packages. In the final stage of refinement, a $CH_2Cl_2$ molecule that came from the solvent mixture of recrystallization was located on the difference Fourier map; the carbon and chlorine atoms were then included in the analysis and refined accordingly. The combined data collection and refinement parameters are given in Table I. Atomic positional parameters for **4** and **5** are presented in Tables II and III, whereas selected bond angles and lengths are given in Tables IV and V, respectively.

## Results and Discussion

Heterometallic phosphinidene clusters have been prepared from the combination of a phosphido complex with organometallic reagents having different metals.[10] Accordingly, we have isolated the phosphinidene starting material $Cp^*WRu_3(CO)_{10}(\mu_3\text{-}H)(\mu_3\text{-}PPh)$ (**3**) from treatment of $Ru_3(CO)_{10}(\mu\text{-}H)(\mu\text{-}PPh_2)$ with excess Cp*W-

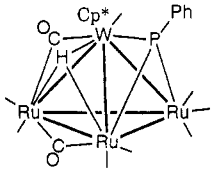

3

**Table I. Experimental Data for the X-ray Diffraction Studies of Complexes 4 and 5**

| compd | **4** | **5** |
|---|---|---|
| formula | $C_{44}H_{40}O_{12}P_2Ru_4W_2$ | $C_{45}Cl_2H_{42}O_{12}P_2Ru_4W_2$ |
| mol wt | 1594.71 | 1679.65 |
| cryst syst | monoclinic | monoclinic |
| space group | $P2_1/n$ | $C2/c$ |
| $a$ (Å) | 12.174(4) | 45.527(5) |
| $b$ (Å) | 17.427(5) | 10.201(1) |
| $c$ (Å) | 22.773(6) | 21.906(9) |
| $\beta$ (deg) | 100.21(2) | 93.90(3) |
| $V$ (Å$^3$) | 4755(2) | 10 150(4) |
| temp (°C) | 25 | 25 |
| $Z$ | 4 | 8 |
| $D_c$ (g/cm$^3$) | 2.228 | 2.198 |
| $F$(000) | 3019.36 | 6366.71 |
| cryst size, mm | 0.08 × 0.40 × 0.50 | 0.30 × 0.50 × 0.55 |
| *hkl* ranges | −13 to +12, 0–18, 0–24 | −48 to +48, 0–10, 0–23 |
| $\mu$ (mm$^{-1}$) | 6.26 | 5.98 |
| no. of unique data | 6195 | 6609 |
| no. of data with $I > 2\sigma(I)$ | 5016 | 5448 |
| no. of atoms (total) | 64 (104) | 67 (109) |
| no. of variables | 578 | 605 |
| $R$; $R_w$ | 0.032; 0.24 | 0.033; 0.029 |
| GOF | 2.16 | 2.01 |

$(CO)_3H$ in refluxing toluene. The derivative 3 reacts with CO in toluene solution at reflux to afford $Cp^*WRu_2(CO)_8(\mu\text{-}H)(\mu_3\text{-}PPh)$ (2).[8] This CO-induced cluster degradation via removal of a $Ru(CO)_3$ fragment was observed in the related $WOs_3$ system.[11] Interestingly, thermolysis of 2 in refluxing toluene led to generation of the two hexanuclear cluster compounds 4 and 5 in 60% and 10% yields, respectively. Both complexes 4 and 5 were purified by chromatography and recrystallization and fully characterized by FAB mass, IR, and $^1H$, $^{13}C$, and $^{31}P$ NMR spectra and single-crystal X-ray diffraction analyses.

**Description of the Structures of 4 and 5.** Compound 4 possesses a hexanuclear core of 2 tungsten and 4 ruthenium atoms coordinated by 12 CO ligands and 2 phosphinidene ligands (Figure 1). The geometry consists of a square-pyramidal $WRu_4$ arrangement with a Ru–Ru edge bridged by a pendant tungsten unit. All metal–metal bonds are normal, with Ru–Ru distances in the range 2.783(1)–3.000(1) Å and W–Ru distances in the range 2.875(1)–3.098(1) Å. One $\mu_3$-phosphinidene ligand occupies a $Ru_3$ metal triangle, and a second $\mu_4$-phosphinidene takes the $WRu_3$ square face. If we consider the $\mu_4$-phosphinidene ligands to be a part of the cluster core, the molecule appears to adopt a $WRu_4P$ octahedral core bridged by a $\mu_3$-phosphinidene and a $Cp^*W(CO)_2$ fragment. The M–P distances of the $\mu_4$-PPh group (2.367(3)–2.428(2) Å) are slightly longer than the metal–phosphorus distances of the $\mu_3$-PPh unit (2.202(2)–2.307(3) Å), which is consistent with the structural features of $\mu_4$-phosphinidenes reported in the literature.[12] Cluster compounds containing both $\mu_4$- and $\mu_3$-phosphinidene ligands have also been characterized.[13]

**Table II. Atomic Coordinates and Equivalent Isotropic Displacement Coefficients for 4**

| | $x$ | $y$ | $z$ | $B_{iso}$, Å$^2$ |
|---|---|---|---|---|
| W(1) | 0.16591(3) | 0.776307(24) | 0.045441(15) | 2.539(17) |
| W(2) | 0.16848(3) | 0.711667(24) | 0.233121(15) | 2.425(17) |
| Ru(1) | 0.26595(6) | 0.65896(4) | 0.13428(3) | 2.11(3) |
| Ru(2) | 0.30869(6) | 0.81064(4) | 0.16930(3) | 2.15(3) |
| Ru(3) | 0.48177(6) | 0.71849(5) | 0.13708(3) | 2.37(3) |
| Ru(4) | 0.38993(7) | 0.83622(5) | 0.05396(3) | 3.11(4) |
| P(1) | 0.33571(21) | 0.70461(15) | 0.05011(9) | 2.75(12) |
| P(2) | 0.47904(21) | 0.84579(15) | 0.14666(10) | 2.68(12) |
| O(1) | 0.0579(5) | 0.7539(3) | 0.15588(22) | 3.0(3) |
| O(2) | 0.1615(6) | 0.9534(4) | 0.0655(3) | 5.6(4) |
| O(3) | 0.0766(6) | 0.5469(4) | 0.2013(3) | 5.6(4) |
| O(4) | 0.3814(6) | 0.6221(4) | 0.2982(3) | 4.6(4) |
| O(5) | 0.1382(6) | 0.5205(4) | 0.0805(3) | 5.4(4) |
| O(6) | 0.4322(6) | 0.5420(4) | 0.1921(3) | 4.5(4) |
| O(7) | 0.2187(7) | 0.9669(4) | 0.1977(3) | 7.2(5) |
| O(8) | 0.4311(5) | 0.7992(4) | 0.29564(23) | 3.6(3) |
| O(9) | 0.6185(6) | 0.6776(4) | 0.2567(3) | 5.9(4) |
| O(10) | 0.6842(7) | 0.6869(5) | 0.0820(4) | 8.3(6) |
| O(11) | 0.3572(8) | 0.9994(5) | 0.0076(4) | 10.0(7) |
| O(12) | 0.5782(7) | 0.8213(5) | −0.0136(3) | 7.4(5) |
| C(1) | 0.1333(6) | 0.7596(5) | 0.1249(4) | 2.4(4) |
| C(2) | 0.1792(9) | 0.8891(6) | 0.0596(4) | 4.3(5) |
| C(3) | 0.1144(8) | 0.6078(6) | 0.2056(4) | 4.1(6) |
| C(4) | 0.3056(8) | 0.6552(5) | 0.2725(3) | 3.1(5) |
| C(5) | 0.1828(8) | 0.5749(5) | 0.1002(4) | 3.2(5) |
| C(6) | 0.3769(8) | 0.5923(5) | 0.1714(4) | 3.0(5) |
| C(7) | 0.2484(8) | 0.9093(6) | 0.1853(4) | 3.8(5) |
| C(8) | 0.3796(6) | 0.7992(5) | 0.2478(3) | 2.4(4) |
| C(9) | 0.5628(7) | 0.6936(5) | 0.2120(4) | 3.1(5) |
| C(10) | 0.6060(8) | 0.6981(6) | 0.1036(4) | 4.2(5) |
| C(11) | 0.3672(10) | 0.9389(7) | 0.0255(5) | 6.3(7) |
| C(12) | 0.5044(9) | 0.8290(6) | 0.0119(4) | 4.9(6) |
| C(25) | 0.0626(7) | 0.6998(5) | −0.0311(4) | 3.1(4) |
| C(26) | 0.0861(7) | 0.7684(6) | −0.0561(3) | 3.2(5) |
| C(27) | 0.0379(9) | 0.8306(6) | −0.0332(4) | 4.5(5) |
| C(28) | −0.0210(8) | 0.8013(5) | 0.0107(4) | 3.7(5) |
| C(29) | −0.0092(7) | 0.7205(6) | 0.0122(3) | 3.9(5) |
| C(30) | 0.0770(8) | 0.6201(6) | −0.0516(4) | 4.5(5) |
| C(31) | 0.1580(9) | 0.7708(7) | −0.1074(4) | 6.2(7) |
| C(32) | 0.0339(10) | 0.9088(6) | −0.0582(5) | 7.0(7) |
| C(33) | −0.0978(8) | 0.8444(7) | 0.0424(5) | 5.7(6) |
| C(34) | −0.0717(8) | 0.6658(7) | 0.0440(4) | 5.2(6) |
| C(35) | 0.0451(7) | 0.7936(6) | 0.2720(3) | 4.2(5) |
| C(36) | 0.1489(8) | 0.8042(5) | 0.3107(4) | 3.8(5) |
| C(37) | 0.1754(9) | 0.7301(6) | 0.3367(4) | 4.1(6) |
| C(38) | 0.0889(8) | 0.6788(6) | 0.3145(4) | 3.9(5) |
| C(39) | 0.0101(7) | 0.7178(6) | 0.2724(4) | 3.5(5) |
| C(40) | −0.0209(10) | 0.8597(7) | 0.2385(4) | 5.8(6) |
| C(41) | 0.2088(9) | 0.8775(6) | 0.3310(4) | 4.9(6) |
| C(42) | 0.2714(9) | 0.7169(7) | 0.3880(4) | 5.8(7) |
| C(43) | 0.0776(11) | 0.6007(7) | 0.3390(4) | 6.2(7) |
| C(44) | −0.1014(8) | 0.6921(7) | 0.2435(4) | 6.0(7) |

Another notable structural feature is concerned with the unique $\mu_4$-$\eta^2$-CO ligand. As illustrated in Figure 1, the C(1)O(1) ligand is encapsulated in the cavity of the $W_2Ru_2$ butterfly with C(1) coordinated to the Ru(1)–Ru(2)–W(1) face and O(1) links to only W(2) atom. The W(2)–C(1) bond (2.565(8) Å) is substantially longer than the opposite W(1)–C(1) bond (1.943(8) Å) and the other two Ru–C(1) distances (Ru(1)–C(1) = 2.369(8) and Ru(2)–C(1) = 2.368(8) Å), indicating that there is either no direct metal–metal bond or only a slight bonding interaction between the W(2) and C(1) atoms. For comparison, the difference of the bond distances between the wingtip metal atoms and the carbon of the $\eta^2$-CO ligand in 4 is near 0.62 Å, while the differences in the butterfly complexes $[Fe_4(\mu\text{-}X)(CO)_{13}]^-$ (X = H, $AuPEt_3$)[14] and $LWRu_3(CO)_{12}(\mu\text{-}H)$ (L = Cp, Cp*)[15] are in the ranges 0.20–0.28 and

---

(10) Landfranchi, M.; Tiripicchio, A.; Sappa, E.; Carty, A. J. *J. Chem. Soc., Dalton Trans.* **1986**, 2737.

(11) Chi, Y.; Lee, G.-H.; Peng, S.-M.; Wu, C.-H. *Organometallics* **1989**, *8*, 1574.

(12) (a) Colbran, S. B.; Johnson, B. F. G.; Lewis, J.; Sorrell, R. M. *J. Chem. Soc., Chem. Commun.* **1986**, 525. (b) Braga, D.; Vargas, M. D. *J. Chem. Soc., Chem. Commun.* **1988**, 1443. (c) Bruce, M. I.; Liddell, M. J.; Skelton, B. W.; White, A. H. *Organometallics* **1991**, *10*, 3282.

(13) (a) Kwek, K.; Taylor, N. J.; Carty, A. J. *J. Am. Chem. Soc.* **1984**, *106*, 4636. (b) Field, J. S.; Haines, R. J.; Mulla, F. *J. Organomet. Chem.* **1990**, *389*, 227.

(14) (a) Manassero, M.; Sansoni, M.; Longoni, G. *J. Chem. Soc., Chem. Commun.* **1976**, 919. (b) Horwitz, C. P.; Holt, E. M.; Brock, C. P.; Shriver, D. F. *J. Am. Chem. Soc.* **1985**, *107*, 8136.

(15) Chi, Y.; Wu, F.-J.; Liu, B.-J.; Wang, C.-C.; Wang, S.-L. *J. Chem. Soc., Chem. Commun.* **1989**, 873.

**Table III. Atomic Coordinates and Equivalent Isotropic Displacement Coefficients for 5**

| | $x$ | $y$ | $z$ | $B_{iso}$, Å$^2$ |
|---|---|---|---|---|
| W(1) | 0.342002(7) | 0.80961(4) | 0.356434(16) | 2.104(16) |
| W(2) | 0.432775(7) | 0.96310(5) | 0.366098(17) | 3.267(20) |
| Ru(1) | 0.395237(14) | 0.80264(9) | 0.28425(3) | 2.47(3) |
| Ru(2) | 0.372694(14) | 1.04291(8) | 0.31838(3) | 2.32(3) |
| Ru(3) | 0.365948(15) | 0.94467(9) | 0.18670(3) | 2.76(4) |
| Ru(4) | 0.317272(14) | 0.98339(8) | 0.25423(3) | 2.34(3) |
| P(1) | 0.34458(4) | 0.7766(3) | 0.24950(10) | 2.41(12) |
| P(2) | 0.32669(5) | 1.0268(3) | 0.35543(10) | 2.42(11) |
| O(1) | 0.40356(11) | 0.8619(7) | 0.42099(24) | 3.0(3) |
| O(2) | 0.44274(13) | 1.1235(9) | 0.2470(3) | 6.4(5) |
| O(3) | 0.46361(13) | 0.7354(9) | 0.3053(4) | 7.5(5) |
| O(4) | 0.41129(15) | 0.5186(8) | 0.3044(3) | 6.0(4) |
| O(5) | 0.43357(12) | 0.8130(9) | 0.1758(3) | 5.6(4) |
| O(6) | 0.37744(15) | 1.2859(8) | 0.2399(3) | 5.5(4) |
| O(7) | 0.38765(16) | 1.2391(9) | 0.4170(4) | 7.3(5) |
| O(8) | 0.37055(14) | 0.7770(9) | 0.0744(3) | 5.9(4) |
| O(9) | 0.40533(15) | 1.1433(9) | 0.1281(3) | 6.3(4) |
| O(10) | 0.31267(14) | 1.0504(10) | 0.1143(3) | 6.8(5) |
| O(11) | 0.25449(12) | 0.8912(8) | 0.2357(3) | 5.9(4) |
| O(12) | 0.29863(14) | 1.2647(8) | 0.2307(3) | 5.8(4) |
| C(1) | 0.38269(16) | 0.8498(9) | 0.3787(3) | 2.5(4) |
| C(2) | 0.43739(18) | 1.0635(11) | 0.2898(4) | 4.0(5) |
| C(3) | 0.44662(18) | 0.8112(11) | 0.3236(4) | 4.2(5) |
| C(4) | 0.40497(20) | 0.6258(11) | 0.2981(4) | 4.3(5) |
| C(5) | 0.41617(17) | 0.8191(11) | 0.2131(4) | 3.9(5) |
| C(6) | 0.37557(17) | 1.1889(10) | 0.2665(4) | 3.2(5) |
| C(7) | 0.38481(20) | 1.1547(11) | 0.3833(4) | 4.0(5) |
| C(8) | 0.36874(18) | 0.8403(11) | 0.1171(4) | 3.7(5) |
| C(9) | 0.39064(18) | 1.0682(11) | 0.1517(4) | 3.8(5) |
| C(10) | 0.32812(19) | 1.0153(12) | 0.1563(4) | 4.5(6) |
| C(11) | 0.27886(18) | 0.9263(11) | 0.2418(4) | 3.4(5) |
| C(12) | 0.30559(18) | 1.1593(11) | 0.2401(4) | 3.5(5) |
| C(25) | 0.32889(18) | 0.5926(10) | 0.3791(4) | 3.0(5) |
| C(26) | 0.34994(17) | 0.6387(10) | 0.4260(4) | 3.0(4) |
| C(27) | 0.33738(19) | 0.7430(10) | 0.4572(4) | 3.4(5) |
| C(28) | 0.30832(17) | 0.7645(10) | 0.4310(4) | 3.4(5) |
| C(29) | 0.30332(18) | 0.6711(10) | 0.3826(4) | 3.2(4) |
| C(30) | 0.33207(23) | 0.4744(12) | 0.3407(5) | 5.3(6) |
| C(31) | 0.37847(20) | 0.5698(12) | 0.4452(5) | 5.0(6) |
| C(32) | 0.35182(21) | 0.8150(12) | 0.5118(4) | 4.5(6) |
| C(33) | 0.28536(20) | 0.8493(11) | 0.4560(5) | 4.9(6) |
| C(34) | 0.27467(21) | 0.6505(13) | 0.3472(5) | 5.7(6) |
| C(35) | 0.48040(20) | 1.0412(17) | 0.3830(4) | 9.0(9) |
| C(36) | 0.47853(21) | 0.9268(17) | 0.4146(6) | 9.2(9) |
| C(37) | 0.46179(21) | 0.9338(15) | 0.4581(5) | 6.6(7) |
| C(38) | 0.44921(18) | 1.0598(13) | 0.4599(4) | 4.8(6) |
| C(39) | 0.46060(20) | 1.1350(13) | 0.4106(5) | 5.6(6) |
| C(40) | 0.5024(3) | 1.057(3) | 0.3377(5) | 19.8(21) |
| C(41) | 0.4990(3) | 0.7996(21) | 0.4121(8) | 13.2(13) |
| C(42) | 0.4551(3) | 0.8257(20) | 0.5056(7) | 12.9(12) |
| C(43) | 0.43021(24) | 1.0994(20) | 0.5097(5) | 11.6(13) |
| C(44) | 0.4591(4) | 1.2706(17) | 0.4012(11) | 20.9(17) |

**Table IV. Selected Bond Distances (Å) and Bond Angles (deg) for 4 (Esd's in Parentheses)**

| | | | |
|---|---|---|---|
| W(1)–Ru(1) | 2.981(1) | W(1)–Ru(2) | 3.098(1) |
| W(1)–Ru(4) | 2.894(1) | W(2)–Ru(1) | 2.875(1) |
| W(2)–Ru(2) | 2.980(1) | Ru(1)–Ru(2) | 2.783(1) |
| Ru(1)–Ru(3) | 2.815(1) | Ru(2)–Ru(3) | 2.847(1) |
| Ru(2)–Ru(4) | 3.000(1) | Ru(3)–Ru(4) | 2.880(1) |
| W(1)–P(1) | 2.401(3) | Ru(1)–P(1) | 2.367(3) |
| Ru(3)–P(1) | 2.428(2) | Ru(4)–P(1) | 2.384(3) |
| Ru(2)–P(2) | 2.307(3) | Ru(3)–P(2) | 2.230(3) |
| Ru(4)–P(2) | 2.202(2) | W(1)–C(1) | 1.943(8) |
| Ru(1)–C(1) | 2.369(8) | Ru(2)–C(1) | 2.368(8) |
| W(2)–C(1) | 2.565(8) | W(2)–O(1) | 2.147(5) |
| C(1)–O(1) | 1.26(1) | | |
| mean W-C(carbonyl) | 2.00(1) | mean Ru–C(carbonyl) | 1.87(1) |

| | | | |
|---|---|---|---|
| W(1)–C(1)–O(1) | 145.6(6) | W(2)–O(1)–C(1) | 94.1(5) |
| Ru(1)–C(1)–Ru(2) | 72.0(2) | mean W–C–O | 168.8(8) |
| Ru(1)–C(6)–O(6) | 168.8(8) | mean Ru–C–O | 175.1(9) |

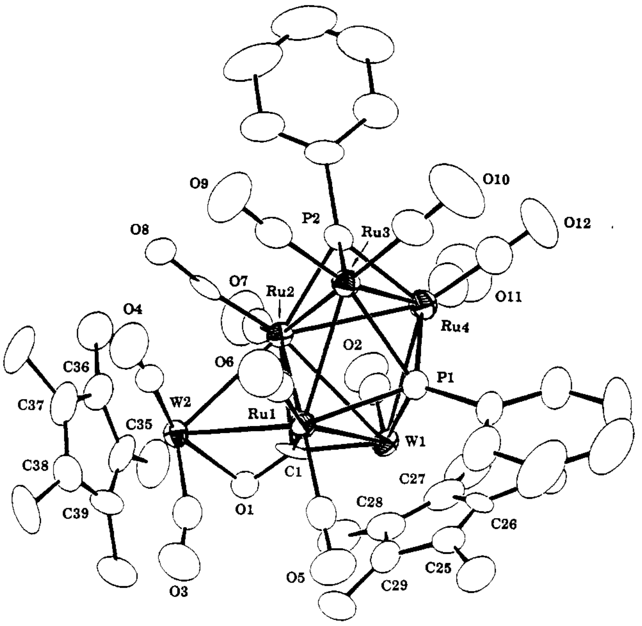

**Figure 1.** Molecular structure of 4 and the atomic numbering scheme.

**Table V. Selected Bond Distances (Å) and Bond Angles (deg) for 5 (Esd's in Parentheses)**

| | | | |
|---|---|---|---|
| W(1)–Ru(1) | 2.984(1) | W(1)–Ru(2) | 2.9102(9) |
| W(1)–Ru(3) | 3.013(1) | W(2)–Ru(1) | 2.898(1) |
| W(2)–Ru(2) | 2.9746(9) | Ru(1)–Ru(2) | 2.779(1) |
| Ru(1)–Ru(4) | 2.838(1) | Ru(2)–Ru(3) | 2.868(1) |
| Ru(2)–Ru(4) | 3.049(2) | Ru(3)–Ru(4) | 2.775(1) |
| W(1)–P(1) | 2.377(2) | Ru(1)–P(1) | 2.394(2) |
| Ru(3)–P(1) | 2.454(3) | Ru(4)–P(1) | 2.442(3) |
| W(1)–P(2) | 2.322(3) | Ru(2)–P(2) | 2.303(2) |
| Ru(3)–P(2) | 2.273(3) | W(1)–C(1) | 1.927(8) |
| Ru(1)–C(1) | 2.237(8) | Ru(2)–C(1) | 2.399(9) |
| W(2)–C(1) | 2.588(8) | W(2)–O(1) | 2.121(6) |
| C(1)–O(1) | 1.286(9) | W(2)–C(3) | 1.94(1) |
| Ru(1)–C(3) | 2.439(8) | Ru(3)–C(10) | 2.259(9) |
| Ru(4)–C(10) | 1.942(9) | W(2)–C(2) | 1.98(1) |
| mean Ru–C(carbonyl) | 1.88(1) | | |

| | | | |
|---|---|---|---|
| W(1)–C(1)–O(1) | 148.5(6) | W(2)–O(1)–C(1) | 95.7(5) |
| Ru(1)–C(1)–Ru(2) | 73.6(2) | W(2)–C(3)–O(3) | 158.2(8) |
| Ru(3)–C(10)–O(10) | 129.0(6) | Ru(4)–C(10)–O(10) | 148.4(7) |
| W(2)–C(2)–O(2) | 173.8(7) | mean Ru–C–O | 174.5(9) |

0.32–0.43 Å, respectively. Another less important feature of CO ligands is that both terminal CO ligands on W(2) adopt a semibridging mode with average angle 168.8(8)°; the unique Ru-bound CO ligand, C(6)O(6), takes a semi triply bridging mode with weak interaction to W(2) and Ru(2) atoms. Finally, assuming that the $\mu_4$-$\eta^2$-CO ligand serves as a four-electron donor, complex 4 contains in total 88 cluster valence electrons, compatible with the prediction of the polyhedral skeletal electron pair theory, in which two of the cluster vertices are nonmetal elements.[16] A few hexanuclear cluster compounds with this kind of $\eta^2$-CO ligand have been documented.[17]

The X-ray diffraction study of 5 was undertaken in an attempt to compare the difference in structure and bonding. An ORTEP diagram is presented in Figure 2, and the corresponding bond distances and angles are given in Table V. The core arrangement is nominally similar to that of 4, comprising an edge-bridged square-pyramidal $WRu_4$ central core, a pendant W metal unit, two phosphinidene ligands, and a $\mu_4$-$\eta^2$-CO ligand which is encap-

---

[16] Mingos, D. M. P. *Acc. Chem. Res.* **1984**, *17*, 311.

[17] (a) Adams, R. D.; Babin, J. E.; Tasi, M. *Inorg. Chem.* **1988**, *27*, 2618. (b) Anson, C. E.; Bailey, P. J.; Conole, G.; Johnson, B. F. G.; Lewis, J.; McPartlin, M.; Powell, H. R. *J. Chem. Soc., Chem. Commun.* **1989**, 442. (c) Johnson, B. F. G.; Lewis, J.; McPartlin, M.; Pearsall, M.; Sironi, A. *J. Chem. Soc., Chem. Commun.* **1984**, 1089.

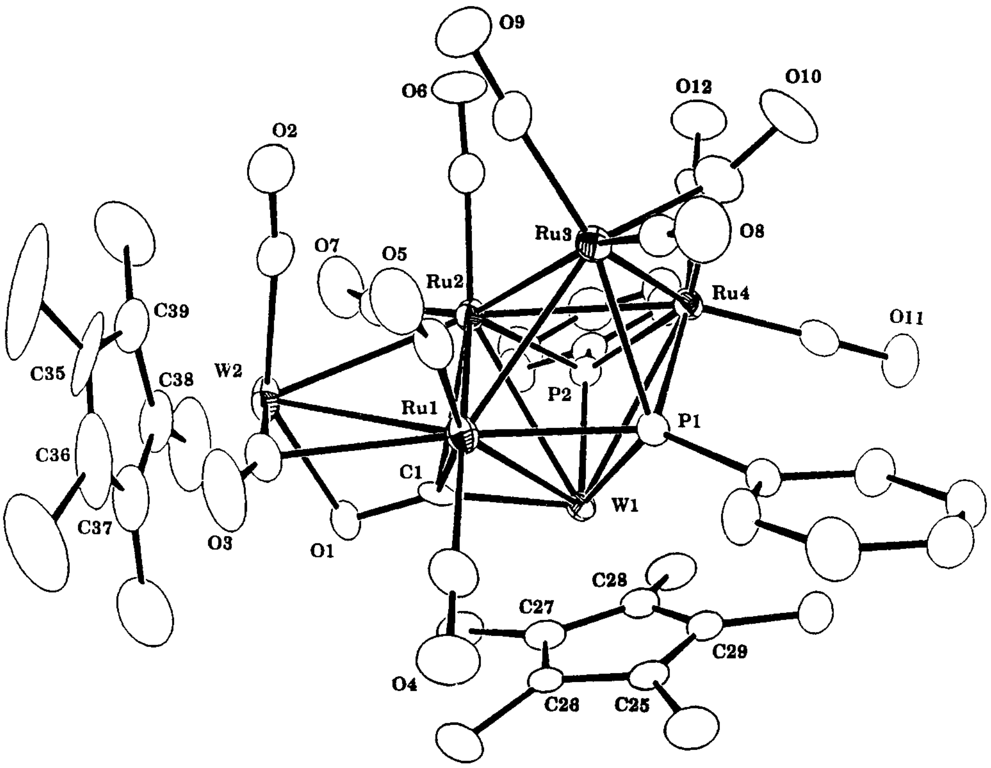

**Figure 2.** Molecular structure of **5** and the atomic numbering scheme.

sulated in the cavity of the $W_2Ru_2$ butterfly. The noteworthy distinction between **4** and **5** is the location of the $\mu_3$-phosphinidene ligand and the disposition of the CO ligands on the metal core. The $\mu_3$-phosphinidene ligand is now coordinated to a $Ru_2W$ face that is adjacent to the $Ru_3$ triangle supporting the $\mu_3$-phosphinidene ligand of **4**. The two carbonyl ligands C(3)O(3) and C(10)O(10) span the Ru(1)–W(1) and Ru(3)–Ru(4) bonds, respectively, and two others, C(5)O(5) and C(7)O(7), adopt semibridging modes with angle $\angle$Ru–C–O $\approx 165°$. Compound **5** is hence related to compound **4** by transferring one phosphinidene ligand from a $Ru_3$ face to the adjacent $WRu_2$ face and by transferring a terminal CO from the W(1) atom to the Ru(3)–Ru(4) edge.

**Characterization by $^{13}$C NMR Spectroscopy.** The $^{13}$C NMR spectrum of **4**, prepared from $^{13}$CO-enriched **2**, displays a series of eight Ru–CO resonances in the high-field region $\delta$ 191.4–213.2 and four W–CO signals at $\delta$ 218.3 ($J_{W-C}$ = 141 Hz), 230.2 ($J_{W-C}$ = 164 Hz), 240.4 ($J_{W-C}$ = 178 Hz), and 280.5 ($J_{W-C}$ = 163 Hz). Assignment of the W–CO ligands is complete. The signal at $\delta$ 218.3 is due to CO on W(1), and the signals at $\delta$ 230.2 and 240.4 belong to the $Cp^*W(CO)_2$ capping fragment. The downfield shift of the last two CO signals is caused by the electron deficiency of the metal atom, because the electron-withdrawing oxygen atom of the $\eta^2$-CO ligand is coordinated to this metal atom. The signal for the $\eta^2$-CO ligand occurs at $\delta$ 280.5 with $^1J_{W-C}$ coupling constant 163 Hz, suggesting that the s character involved in the W–C bonding is similar to that for the terminal W–CO ligands. The observed chemical shift of the $\eta^2$-CO ligand is compatible with those observed in butterfly complexes $[Fe_4(\mu\text{-}X)(CO)_{13}]^-$ (X = H, $AuPPh_3$, $HgCH_3$) ($\delta$ 284.9–279.8)[18] and $LWRu_3(CO)_{12}(\mu\text{-}AuPPh_3)$ (L = Cp, Cp*) ($\delta$ 272.8–255.1).[19]

For complex **5**, the $^{13}$C NMR spectrum recorded at 213 K shows the $\eta^2$-CO signal at $\delta$ 267.8 ($J_{W-C}$ = 175 Hz), two terminal W–CO signals at $\delta$ 246.4 ($J_{W-C}$ = 183 Hz) and 219.6 ($J_{W-C}$ = 147 Hz), one CO bridging a Ru–Ru bond at $\delta$ 234.2, and eight terminal Ru–CO resonances in the range $\delta$ 218.8–183.8. When the temperature was raised to 294 K, the Ru–CO signals at $\delta$ 234.2, 202.2, and 183.8 broadened and coalesced into the base line, indicating rapid exchange between these CO ligands. As the downfield signal at $\delta$ 234.2 is assigned to the bridging CO ligand, the observed fluxional process may be due to a localized exchange involving the bridging CO and the two CO groups linked to atom Ru(4); the bridging CO interacts more strongly with the Ru(4) atom, because the Ru(4)–C(10)–O(10) angle (148.4°) is slightly larger than the Ru(3)–C(10)–O(10) angle (129.0°). Furthermore, the resonance at $\delta$ 202.2 is assigned to the CO located trans to atom P(2), because this signal exhibits a large $J_{P-C}$ coupling of 35 Hz.

**Selective $^{13}$C Enrichment of Terminal CO Ligands.** The CO exchange experiments provide qualitative information about the coordination strength of the $\eta^2$-CO ligand. Heating the solution of **4** under 1 atm of $^{13}$CO (100 °C, 12 h) produced a sample having selective enrichment, which contains a $\eta^2$-$^{12}$CO group and 11 terminal $^{13}$CO ligands. This result is confirmed by the $^{13}$C NMR spectrum, which displays only 11 signals due to terminal CO ligands and no $\eta^2$-CO signal at $\delta$ 280.5. This observation is fully consistent with the expectation the $\eta^2$-CO ligand interacts more strongly with the cluster core due to the additional bonding interaction between tungsten and oxygen atoms. However, loss of the $\eta^2$-$^{12}$CO label takes place at higher temperature. This effect is illustrated by the detection of all 12 CO resonances with equal intensity in the $^{13}$C NMR spectra of both **5** and recovered **4**, obtained from further heating of the selectively $^{13}$CO enriched sample of **4** (110 °C, 7 h).

---

[18] (a) Horwitz, C. P.; Shriver, D. F. *Organometallics* **1984**, *3*, 756. (b) Horwitz, C. P.; Shriver, D. F. *J. Am. Chem. Soc.* **1985**, *107*, 8147.

[19] Cheng, C.-C.; Chi, Y.; Peng, S.-H.; Lee, G.-H. Unpublished results.

**Scheme I**[a]

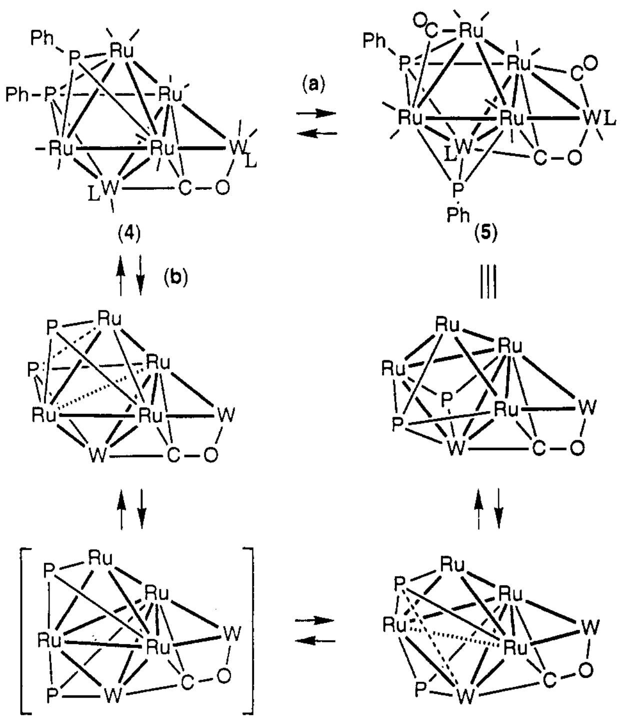

[a] The bonds being broken and formed are indicated by dashed lines.

**Reactivity Studies.** A delicate equilibrium between compounds 4 and 5 at higher temperature is implicated because heating a solution of 4 under reflux in toluene for 2 h provided a mixture of 4 and 5 in 69% and 19% yield, respectively. Similarly, the isomerization is established from the opposite direction, as thermolysis of pure 5 under identical conditions regenerates a mixture of 4 and 5 in 13% and 80% yield, respectively. A likely mechanism involves the direct migation of the $\mu_3$-PPh ligand from the $Ru_3$ face to the $WRu_2$ face (pathway **a** in Scheme I); in this case, the $\mu_4$-PPh ligand does not participate in the cluster core rearrangement. The isomerization may alternatively pass through a trigonal-bipyramidal $WRu_4$ intermediate, which is obtained by cleavage of the Ru(1)–Ru(4) bond and formation of the P(1)–Ru(3) linkage (also see pathway **b** in Scheme I). This intermediate would have a W atom in an apical position and two $\mu_3$-PPh groups; one attaches to the $Ru_3$ triangular face and the second to the $WRu_2$ face. Subsequent formation of 5 is expected if the Ru(2)–Ru(4) bond in the trigonal-bipyramidal intermediate is broken and concurrently the bond between P(2) and W(1) is formed. In this case the $\mu_3$-PPh and $\mu_4$-PPh groups have exchanged their positions; thus, it can be differentiated from the first proposed pathway. We cannot delineate the exact pathway for the interconversion without acquiring more experimental data.

A detailed analysis of the reaction mechanism is also hampered by the low yield of the interconversion and the unwanted retardation effect of the CO atmosphere. Thermolysis of 4 under 1 atm of CO reduced the yield of 5 from 19% to 7%, compared to the reactions carried out under an $N_2$ atmosphere; further increase of the pressure to 2 atm lowered the isolated yield to approximately 3%. The reduction in the yields implies that the isomerization is inhibited by CO; however, the validity of this statement is disputable because of the observation of severe, concomitant cluster decomposition. For the same reason, no attempt was made to further explore these CO inhibition experiments.

Furthermore, the CO atmosphere has another notable effect of promoting degradation of clusters. For example, heating of 4 in toluene under CO at 4 atm (100 °C, 12 h) failed to produce any complex 5 in significant quantity but led to isolation of the two homonuclear diphosphinidene clusters $Ru_3(CO)_9(\mu_3\text{-PPh})_2$ (6; 37%) and $Ru_4(CO)_{11}(\mu_4\text{-PPh})_2$ (7; 30%), which were identified by comparison of their spectral data with those reported in the literature.[20] Unlike the reactions with CO, dihydrogen reacts to afford small amounts of 2 and 3 within 1 h. It is apparent that the dihydrogen molecule serves as a source of hydrides in regeneration of smaller clusters 2 and 3.

**Conclusion.** The most interesting finding of this work is the isolation of hexanuclear $W_2Ru_4$ clusters that result from the coupling of trinuclear phosphinidene clusters. Also remarkable is the presence of the $\eta^2$-CO ligand, which serves as a support to the pendant $Cp^*W(CO)_2$ unit and has a slightly higher energy barrier with respect to the exchange with free CO molecules. Reactions with CO or $H_2$ lead to the destruction of the metal cluster in which the conditions and reagents employed control the final isolable products.

**Acknowledgment.** This research was supported by the National Science Council of the Republic of China (Grant No. NSC 82-0208-M007-079).

**Supplementary Material Available:** Tables of additional crystal data and structure solution and refinement details, nonessential bond distances and angles, positional parameters of phenyl rings and calculated positions of hydrogen atoms, and anisotropic thermal parameters for 4 and 5 (18 pages). Ordering information is given on any current masthead page.

OM930268H

---

(20) Field, J. S.; Haines, R. J.; Smit, D. N. *J. Chem. Soc., Dalton Trans.* 1988, 1315.